

# Preparation and Identification of Magnetic Iron Nanoparticle based on a Natural Hydrogel and its Performance in Targeted Drug Delivery

Vahid Hosseini<sup>1</sup>; Seyed Masoud Ghoreishi Mokri<sup>2</sup>; Dalia hafezghoran<sup>3</sup> Bahareh Karimi<sup>4</sup>  
Anastasia Aleksandrovna Anashkina<sup>5</sup>; Anna Borisovna Yazykova<sup>6</sup>

<sup>1</sup>Dentistry student at Privolzhsky Research Medical University, Nizhny Novgorod, Russia

<sup>2</sup>Department of Medicine at Privolzhsky Research Medical University, Nizhny Novgorod, Russia

<sup>3</sup>General medicine department of Privolzhsky Research Medical University

<sup>4</sup>Dentistry department of Privolzhsky Research Medical University

<sup>5</sup>PhD, the Head of the Biochemistry Department of Privolzhsky Research Medical University

<sup>6</sup>Phd, Senior Professor of Biochemistry Department of Privolzhsky Research Medical University

**Abstract:-** Billions of dollars are spent annually in the world to treat and investigate problems caused by drug side effects. According to the estimates of health researchers, about 40% of people who take medicine suffer from side effects. In this way, the necessity of using a targeted system in order to deliver medicine to the desired place without damaging healthy tissues is felt more than ever. In recent years, targeted drug delivery systems based on nanoparticles have received much attention. Meanwhile, the use of natural polymers is more suitable for various purposes in drug delivery systems in terms of indicating greater biological compatibility with the body and being non-toxic.

In this research, the natural hydrogel extracted from the seeds of the *Plantago ovata*, which is loaded on the bed of magnetic iron nanoparticles, was used to entrap the drug mefenamic acid. In order to achieve this goal, at the beginning, magnetic iron nanoparticles were prepared by co-precipitation method using iron (II) and iron (III) oxides, and then a coating of silica was created on its surface, then the hydrocolloid of *Plantago ovata* was extracted from its seed, in order to connect the magnetite nanoparticles and the polymer extracted from the *Plantago ovata*, the surface of both components was modified by vinyl-functional groups. Next, radical polymerization under heat was used to connect the particles and trap the drug, after that the release of the drug from the polymer capsule was checked by UV-Vis device. Before examining the drug release, the resulting product was identified by FT-IR, XRD, VSM, DLS, TGA, SEM analysis. Therefore, the obtained results indicated that the natural polymer was correctly loaded on the desired magnetic substrate and the drug mefenamic acid was trapped inside the hydrogel networks and polymer capsule. Therefore, the drug can be directed in a controlled and targeted manner by the magnetic field, and the release of the drug was done well and at an acceptable speed.

**Keywords:-** Targeted Drug Delivery, Natural Hydrogel, Magnetic Nanoparticles, *Plantago Ovata*.

## I. INTRODUCTION

Medicine is considered an important factor in the prevention and treatment of diseases, which is one of the main treatment methods along with surgery, physical therapy, radiation, etc. Considering the increase in the annual consumption of drugs in the world and the involvement of more people with side effects caused by the use of drugs, nowadays the necessity of using a system that can control the speed, time and place of release of the drug after entering the body is felt very much. These systems, which are growing in different forms, help a lot to improve the effect of drugs and reduce their side effects. Targeted drug delivery systems (DDS) play a very important role in the pharmacological effects of drugs. These systems, in addition to the effect they have on the loading, release and distribution of the drug at the site-of-action, can affect the biological properties expected from the drug. In general, DDS systems guarantee the correct placement of the drug in the desired site and the controlled release of the drug in that site [1-3].

Encapsulation is a technique that uses that ingredient or a combination of ingredients to be coated by another system. The coated ingredient is called active ingredient or core, and the coating material is called carrier or encapsulant. In recent years, this technique has progressed and grown a lot in scientific and industrial societies. This method can be used to improve efficiency, increase stability, increase the compatibility of the active ingredient, increase safety, and also be used as a carrier in the targeted delivery of ingredient [4].

### A. The Purpose of the Research

Considering that so far there has been no report on the use of targeted drug delivery systems on the mefenamic acid drug using a natural hydrogel, therefore, in this project, using iron nanoparticles and hydrogel extracted from the *Plantago ovata*, it was tried to check the possibility of loading this drug in the networks of a natural magnetized polymer and also the release rate of the drug in simulated conditions of the body in the laboratory environment.

### B. Characteristics of the *Plantago ovata* and the natural hydrogel extracted from it

*Plantago ovata* belongs to the family of Plantaginaceae, this plant is native to parts of Asia, Mediterranean and North Africa and is mainly found in Iran, India and Pakistan. *Plantago ovata* seed is almost boat-shaped and has a brownish color, by grinding its seed, *Plantago ovata* bran is obtained [5-6].



Fig 1: *Plantago Ovata* Seed

Among the natural polysaccharides that have recently been studied and studied in the field of hydrogel and drug delivery, the hydrogel extracted from *Plantago ovata* bran has been one of the most promising; A functional and lightweight polymer that is easily available at low cost [7].

### C. Nanoparticles in Targeted Drug Delivery Systems

Drug delivery systems based on nanoparticles have been widely used in recent years. The pattern of using drug carriers in the body environment in order to increase the efficiency and reduce the degradation of the drug, prevent the side effects caused by the use of the drug and increase the access to the drug and improve its effect at the lesion site was investigated and used, and many pharmaceutical researches and clinical studies were conducted on this topic [8].

In a general definition, it can be said that the particles whose size is in the range of (10-100) nanometers are called nanoparticles. Nanoparticles, due to their very small size and high surface-to-volume ratio, can be used to connect multiple ligands to the surface due to their tendency to create multiple covalent bonds. Other characteristics of nanoparticles include chemical and biological stability, the possibility of binding to both hydrophilic and hydrophobic drugs, and the ability to be prescribed by different routes such as oral, inhalation and injection [9]. These nanoparticles have the ability to carry the drug in a dissolved, trapped, encapsulated or attached to the nanoparticle matrix [10].

## II. CLASSIFICATION OF NANOPARTICLES USED IN TARGETED DRUG DELIVERY SYSTEMS

The types of nanoparticles used in drug delivery as drug carriers can be divided into several categories based on their constituent materials:

### A. Nanoparticles of Inorganic Origin

From this category, we can mention magnetic nanoparticles, carbon spheres, silicate mesoporous particles and gold nanoparticles, which can play a role depending on the purpose.

#### ➤ Magnetic Iron Nanoparticles

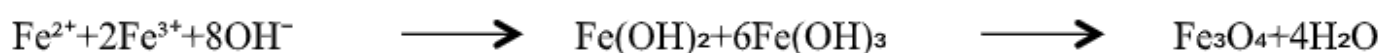
A group of nanoparticles that have an inorganic origin and are widely used in drug delivery systems are magnetic iron nanoparticles that are chemically or biologically synthesized. Due to their magnetic properties, these particles can be directed to the specific desired site (site of action) in the body by an external field, therefore, they are very useful and important in the field of targeted drug delivery. From this category, we can mention magnetite and maghemite nanoparticles, which have received a lot of attention in drug delivery. One of the most important advantages of magnetic nanoparticles is that their surface can be easily modified.

#### ➤ Preparation Methods of Magnetic Nanoparticles

In recent years, many methods have been designed and introduced for the production of magnetic nanoparticles, and in most of them, the focus is on obtaining a controlled shape, high stability and size of nanoparticles. The method used for the synthesis of magnetic nanoparticles depends on the type of properties of the desired material, which can be chosen after determining the properties of the desired product according to the shape, distribution and economic aspects. Among the methods that have been designed so far, we can mention sol-gel method, co-precipitation method, hydrothermal, combustion, sonochemical and microemulsion [12-13].

#### ➤ Co-Precipitation Method to Prepare Magnetic Nanoparticles

It is one of the oldest methods of synthesis of magnetic nanoparticles, which was used for the first time to produce magnetite nanoparticles. One of the advantages of this method is its single step, ease, cost-effectiveness and speed, which produces a fine and uniform product. In this method, iron (II) and iron(III) oxides and a base are used and magnetite nanoparticles can be synthesized. Among the effective parameters in the production of these nanoparticles, we can mention the ionic strength, the type of salt used, the reaction temperature, pH, the speed of stirring the reaction and adding base, and the ratio of iron (II) and iron (III) ions, which are different in size and shape. The composition of synthesized nanoparticles is effective [14].



### B. Nanoparticles of Polymer Origin

Polymeric nanoparticles have been widely used in drug delivery. One of the characteristics of polymers used in this field is their biocompatibility and non-toxicity. The advantages that this category of nanoparticles have over others is the ability to synthesize them in large quantities and also their stability. Polymer particles are divided into two categories: homopolymers and copolymers, micelles and polymersomes in the copolymer category, and on the other hand nanocapsules, nanospheres, dendrimers and nanogels are included in the homopolymer category [10].

#### ➤ Hydrogels

For the first time in the early 1960s, Lim and Wichterle began their biological studies on a hydrophobic gel. After that, until today, many efforts and studies have been devoted to the development and expansion of the capabilities of hydrogels [14]. In general, hydrogels can be called polymer networks with a three-dimensional configuration that have transverse connections and are able to absorb large amounts of water or biological fluids [10-15].

The ability of hydrogel to absorb water is due to the presence of hydrophilic groups such as  $\text{SO}_3\text{H}$ ,  $\text{OH}$ ,  $\text{CONH}$  and  $\text{CONH}_2$  in the structure of the constituent monomers, depending on the contribution of these groups and the nature of the aqueous environment and polymer composition, the hydrogel can have different degrees of hydration. Sometimes it reaches 90% of the weight of the gel. On the other hand, there are also hydrophobic polymer networks, such as polylactic acid (PLA) or Poly lactic- co-glycolic acid (PLGA), which have a low water absorption capacity (about 5-10%). The water content that can be absorbed by the hydrogel determines its unique chemical and physical properties. The fully swollen hydrogel has physical properties in common with living tissues, including its soft and elastic texture and interfacial tension with water and other biological body fluids. Due to their high water absorption power, hydrogels swell instead of dissolving in water and therefore acquire elastic properties, which minimizes the irritation of the tissues around the hydrogel after implantation. The low interfacial tension between the surface of the hydrogel and body fluids reduces protein absorption and cell adhesion, which reduces the body's negative reaction. In addition to the mentioned advantages, the pores in the hydrogel create the ability to contain the drug and therefore can be used as a drug delivery system. In this context, hydrogels can be used in the form of nanoparticles, microparticles, pieces and films [10,16].

The reason why the gel does not dissolve in water is the presence of transverse connections between the polymer chains that make up the hydrogel, these stable connections may be in the form of covalent bonds or in the form of non-covalent physical bonds such as ionic bonds, hydrogen bonds, hydrophobic bonds and physical interweaving [17].

### III. MEFENAMIC ACID DRUG PROPERTIES

It is a non-steroidal anti-inflammatory drug and an anthranilic acid derivative. By reducing the necessary enzymes, mefenamic acid inhibits the production of prostaglandins and disrupts their action at the receptor site. The half-life of mefenamic acid drug is 2 hours and it has analgesic, anti-inflammatory and anti-pyretic properties. It is also a drug that is poorly soluble in water.

#### ➤ Side Effects of High Consumption of Mefenamic Acid

Among these complications, we can mention problems and disorders of the digestive system, reactions and skin lesions, serious allergic reactions, vision disorders, liver and kidney problems, and it can also be a factor in reducing the amount of red blood cells and as a result, anemia. It also causes drug interactions with some drugs [18].

### IV. RESEARCH FINDINGS

The steps of preparing the final product ( $\text{Fe}_3\text{O}_4@\text{SiO}_2@\text{Poly}@\text{drug}$ ) include 5 main steps, which are explained below.

#### A. Preparation of Magnetite Nanoparticles (MNPs)

Co-precipitation method was used for the synthesis of nanoparticles in this research. For this purpose, 4.5 grams of  $\text{FeCl}_3 \cdot 6\text{H}_2\text{O}$  and 2 grams of  $\text{FeCl}_2 \cdot 4\text{H}_2\text{O}$  in 100 ml of double distilled water were added to a fume hood equipped with nitrogen inlet and outlet, the resulting mixture was vigorously stirred with a magnetic stirrer under reflux conditions and a temperature of  $85^\circ\text{C}$  for 15 minutes. Then 15 ml of 30% ammonia solution was added drop by drop to the mixture, the color of the mixture immediately changed from orange to black. The resulting solution was refluxed for 30 minutes. After the end of the reaction, the precipitate was separated by a magnet and washed 3 times with double distilled water. The black precipitate of  $\text{Fe}_3\text{O}_4$  resulting from this step was identified by FT-IR, VSM and SEM analyses.



Fig 2: Magnetite Preparation Reaction



➤ *Mechanism of Formation and Identification of Magnetite Nanoparticles (Fe<sub>3</sub>O<sub>4</sub>)*

To prepare these nanoparticles, a co-precipitation method was used, in which iron (II) and iron (III) salts were

used with stoichiometric ratios of 1 to 2 according to the following reaction:



By adding ammonia to the reaction solution containing iron salts, spherical and black iron nanoparticles are obtained as shown in Figure 3:

Magnetic iron nanoparticles oxidize when exposed to air and produce Fe(OH)<sub>3</sub> according to the reaction shown below. To prevent oxidation, nanoparticles were synthesized in the presence of nitrogen gas.

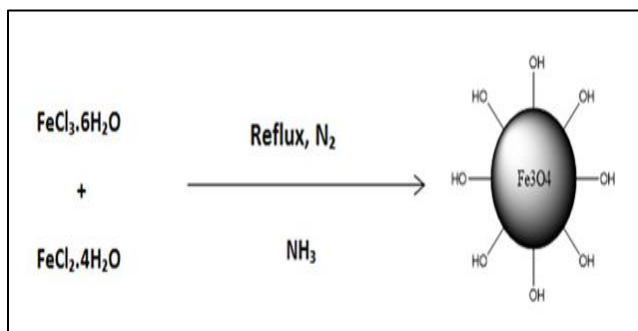


Fig 3: General Scheme of Preparation of Magnetite Nanoparticles



➤ *Investigation Infrared (FT-IR) Pattern Obtained from Fe<sub>3</sub>O<sub>4</sub> Nanoparticles*

Diagram 1 shows the FT-IR spectrum obtained from the prepared Fe<sub>3</sub>O<sub>4</sub> compound. The two bands appearing at 430Cm<sup>-1</sup> and 560Cm<sup>-1</sup> correspond to the vibrations of the Fe—O bonds of the compound. The band related to surface OH groups can also be seen in the range of 3400Cm<sup>-1</sup>.

have a small amount of magnetic moment. In the ferromagnetic state, the atomic magnetic moments have the same orientation relative to each other. Therefore, the crystal lattice has a total magnetic moment. This is despite the fact that in an antiferromagnetic crystal, half of the atomic magnetic moments are directed upwards and the other half are directed downwards. Therefore, the total magnetic moment for an antiferromagnetic crystal is zero. Figure 4 shows the magnetization diagram of a ferromagnetic material with magnetic strength M in the presence of an external magnetic field with strength H. As it can be seen, with the increase of H, the amount of M increases until it reaches its highest level, which is called the saturation magnetization of MS. The resulting diagram shows a residual magnetic value after removing the external field, which is called "residual ring". The presence of this ring indicates that after the removal of the external magnetic field, some magnetic property remains in the material and all the magnetic property of the ferromagnetic material is not lost. Because after the removal of the external magnetic field, the orientation of the atomic magnetic moments in all areas do not return to their original arrangement. Therefore, even when the value of the external field H reaches zero, there is still some remnant magnetization MR in the material, which can only be destroyed by applying a coercive field HC, against the direction of the initial field. In the magnetization diagram of single-domain magnetic materials, no residual loop is observed, such compounds are called super-para- magnetic. Magnetite nano-oxides with a size smaller than 100 nm have superparamagnetic properties at room temperature [19].

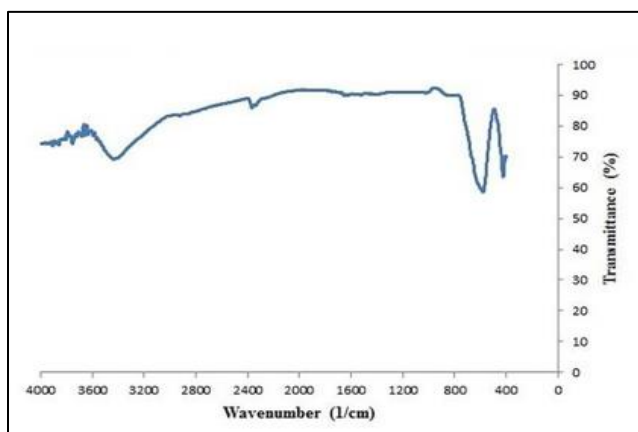


Diagram 1: FT-IR Spectrum of Magnetite Nanoparticles

➤ *Examining the Results of the Magnetometric Test (VSM) of Fe<sub>3</sub>O<sub>4</sub> Nanoparticles*

In paramagnetic materials, the arrangement of atomic magnetic moments is completely random and separate, so that the magnetic moment of the entire crystal lattice is zero. In this case, if these materials are exposed to an external magnetic field, some of these separate atomic magnetic moments will find the same orientation and the network will

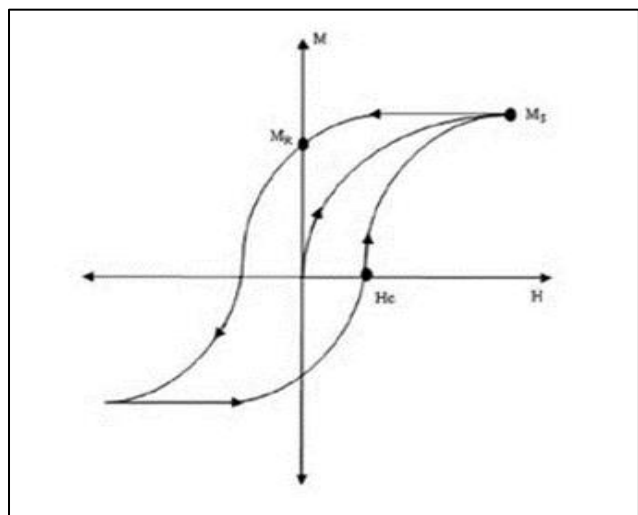


Fig 4: Changes of Magnetization in a Ferromagnetic Material

Diagram 2 shows the magnetic behavior of magnetite nanoparticles, which was investigated by performing vibrational magnetometric analysis of the VSM sample. As can be seen, the obtained magnetite particles show the characteristic of superparamagnetism with a maximum magnetization of 70 emu/g. The absence of a residual loop in the magnetization diagram is a confirmation of the superparamagnetic behavior of magnetite in the presence of an external magnetic field.

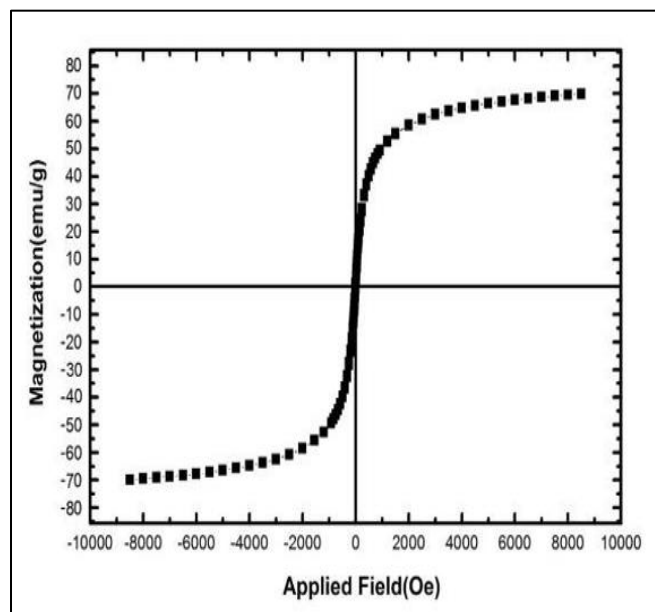


Diagram 2: Magnetometric Diagram of Magnetite Nanoparticles

➤ *X-Ray Diffraction (XRD) Pattern Investigation Of Fe<sub>3</sub>O<sub>4</sub> Nanoparticles*

The X-ray diffraction pattern of Fe<sub>3</sub>O<sub>4</sub> compound is shown in Figure 5. Comparing this pattern with the reference magnetite pattern in the above device with JCPDS No. 19-0629, which belongs to Fe<sub>3</sub>O<sub>4</sub>, determined that all the diffraction signals related to the prepared magnetite structure are consistent with the diffraction related to the reference magnetite structure in terms of the position and intensity of vibrations, which is a confirmation of the formation of the Fe<sub>3</sub>O<sub>4</sub> compound.

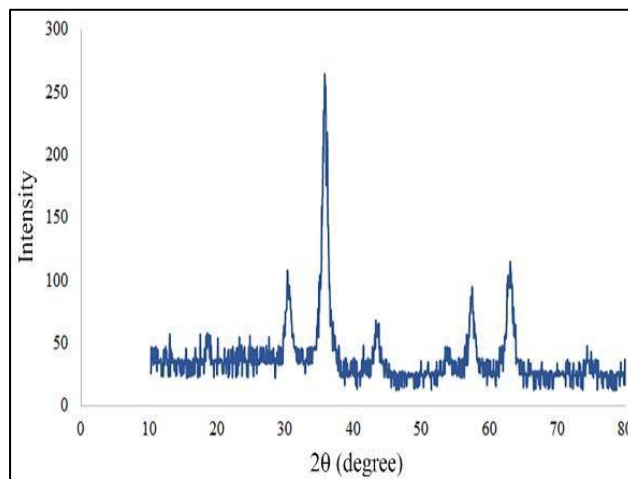


Fig 5: X-ray Diffraction Pattern of Magnetite Nanoparticles

➤ *Examining the Scanning Electron Microscope (FE-SEM) Images Obtained from Fe<sub>3</sub>O<sub>4</sub> Nanoparticles*

Scanning electron microscope is used to determine surface morphology, texture, size and shape of major samples of solid materials. The FE-SEM images obtained from the Fe<sub>3</sub>O<sub>4</sub> compound in this project are shown in Figure 6. As can be seen, the obtained nanoparticles are assemblies of spherical particles stuck together with a high surface area and an approximate size of 20-30 nm.

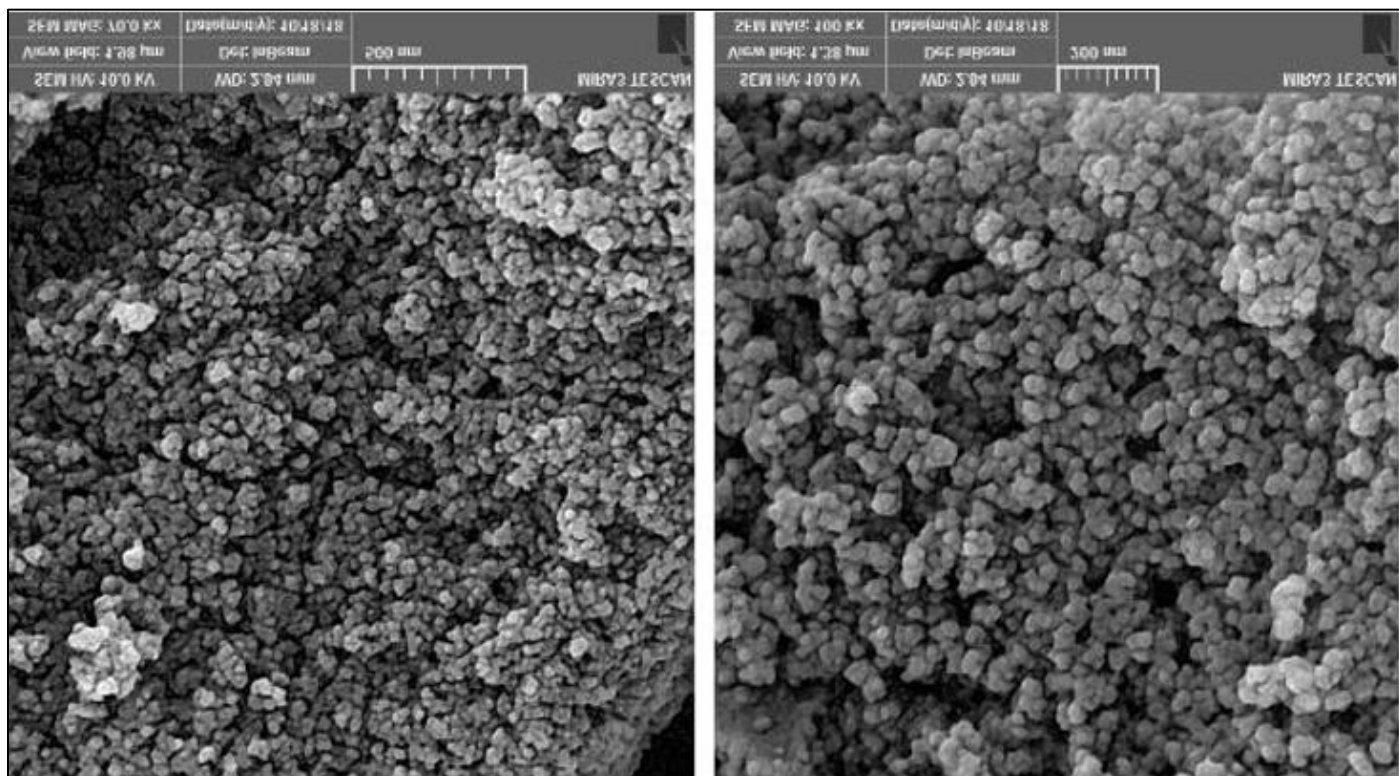


Fig 6: FE-SEM Images Obtained from Magnetite Nanoparticles

#### B. Preparation of Silica Coated Iron Nanoparticles ( $Fe_3O_4@SiO_2$ )

Silica coated magnetic nanoparticles were prepared with a slight modification according to Liu et al.'s method (20). In this step, 3 grams of  $Fe_3O_4$  nanoparticles obtained from the previous step were transferred to a double-mouth flask and 80 ml of tetraethyl orthosilicate (TEOS) solution of 10% by volume in deionized water was added to it. After that, 60 ml of glycerol was added to the mixture and the pH of the resulting suspension was adjusted by acetic acid to about 4.5. At the end, the resulting mixture was stirred under reflux at a temperature of 90°C for 2 hours with a magnetic stirrer. At the end, the resulting contents were transferred to a beaker, the sediment was separated by a magnet, and washed with double distilled water and methanol, respectively. After drying at room temperature, the resulting nanoparticles were identified by FT-IR spectroscopy.

#### ➤ Mechanism of Formation and Identification of Silica Coated Magnetic Iron Nanoparticles ( $Fe_3O_4@SiO_2$ )

In order to prevent magnetite nanoparticles from oxidizing, an ineffective layer of silica is placed between the iron core and the reaction medium. It is possible to perform this operation with the sol-gel technique and by adding the TEOS compound to the solution containing magnetite nanoparticles [21].

Among the effects of silicon coating on magnetite nanoparticles, we can mention protecting them against oxidation, creating a suitable space for modifying the surface of nanoparticles, and also increasing their thermal stability. Another important advantage of this process is the increase in the number of hydroxyl groups on the surface of nanoparticles, which causes better functionalization on the surface of nanoparticles. Also, the silica coating prevents the clumping of nanoparticles and the distribution of particles in the solution environment is better [22].

The mechanism of this process is shown below in Figure 7. First, TEOS molecules are formed in the vicinity of glacial acetic acid and glycerol hydrolysis, followed by hydroxyl groups. Adding glycerol to the solution causes the nanoparticles to be completely separated and the silica coating is done more effectively. The reason for adding acid is to adjust the pH of the solution in order to hydrolyze the OH groups on the surface of nanoparticles and TEOS molecules, and as a result, these molecules are effectively connected to each other.

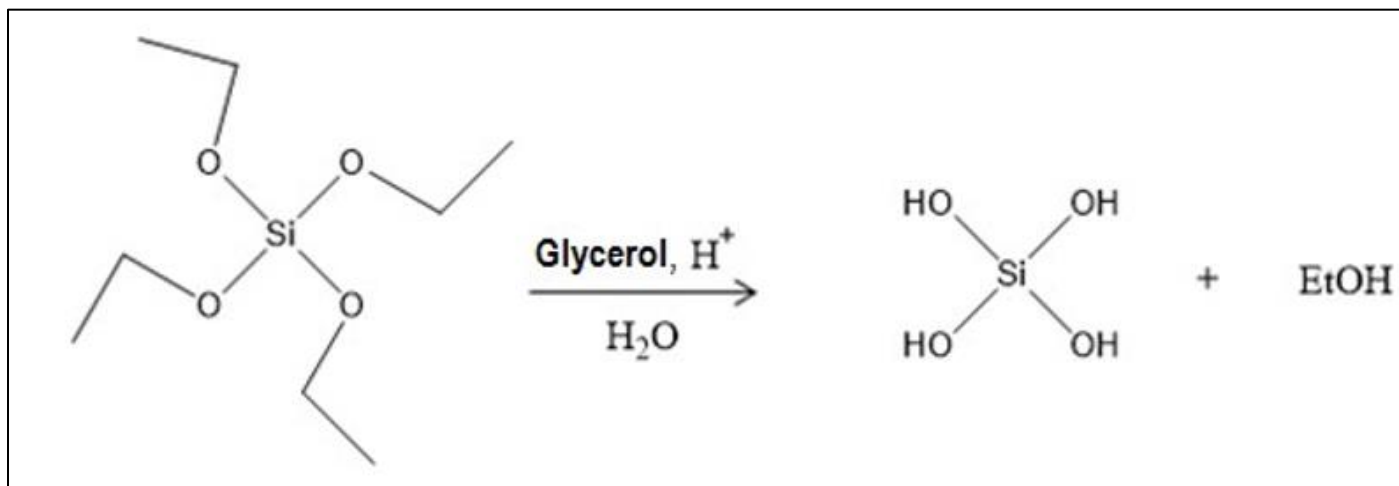


Fig 7: Hydrolysis Mechanism of TEOS Molecules

A scheme of the process of creating silica coating on magnetite nanoparticles is shown in Figure 7:

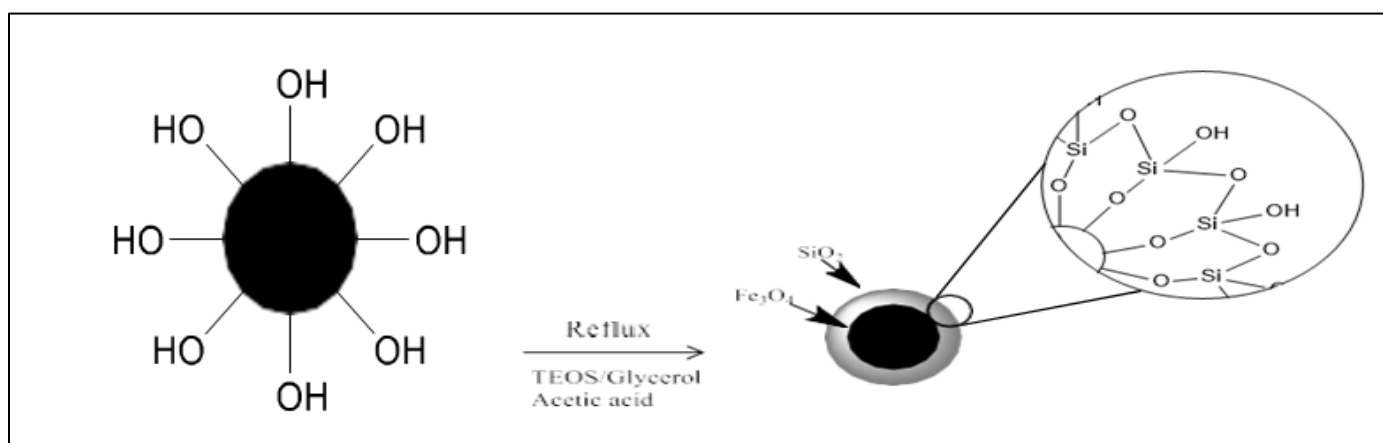


Fig 8: A Plan of the Silicon Coating Process of Magnetite Nanoparticles

➤ *Investigating the Infrared Pattern (FT-IR) Related to (Fe<sub>3</sub>O<sub>4</sub>@SiO<sub>2</sub>)*

Figure 7 is the FT-IR spectrum of silica coated magnetite nanoparticles. All bands related to the previous stage are observed in this spectrum. Vibrations related to Fe—O bonds appeared in the range of  $\text{Cm}^{-1}460$ , which overlapped with the bands related to Fe—O—Si bonds located in this range. For this reason, the existence of a silicon network on the surface of nanoparticles is proved by the bands related to the symmetric and asymmetric stretching vibrations of the Si—O—Si bond, which appeared in the range of  $980\text{Cm}^{-1}$  and  $1080\text{Cm}^{-1}$ , respectively (23). The broad band appearing in the range of  $3400\text{Cm}^{-1}$  indicates the presence of OH bonds on the surface of these nanoparticles (24).

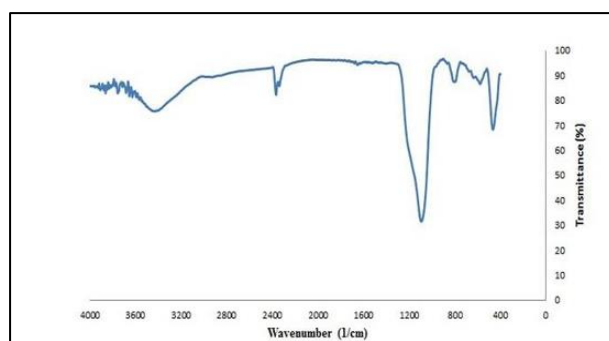


Diagram 3: FT-IR Spectrum of Silica Coated Magnetite Nanoparticles

C. *Preparation of Fe<sub>3</sub>O<sub>4</sub> Nanoparticles Functionalized by Trimethoxyvinyl Silane Groups (Fe<sub>3</sub>O<sub>4</sub>@SiO<sub>2</sub>@Vinyl)*

To functionalize Fe<sub>3</sub>O<sub>4</sub> nanoparticles by trimethoxyvinyl silane (VTMOS) groups, 3 grams of SCMNP obtained from the previous step were placed in 50 ml of absolute ethanol for 10 minutes in an ultrasonic bath. Then 10 ml of VTMOS was added drop by drop to the obtained suspension. The pH of the mixture was adjusted by glacial acetic acid at about 4.5 and refluxed for 24 hours. After cooling, the resulting mixture was separated by an external magnetic field and the sediment obtained was washed with



ethanol to remove the residual trimethoxyvinyl silane. The resulting precipitate was dried in an oven at a temperature of 70°; and it was identified by FT-IR spectroscopy.

In Figure 9, a summary of the functionalization steps of  $Fe_3O_4$  nanoparticles is shown schematically below:

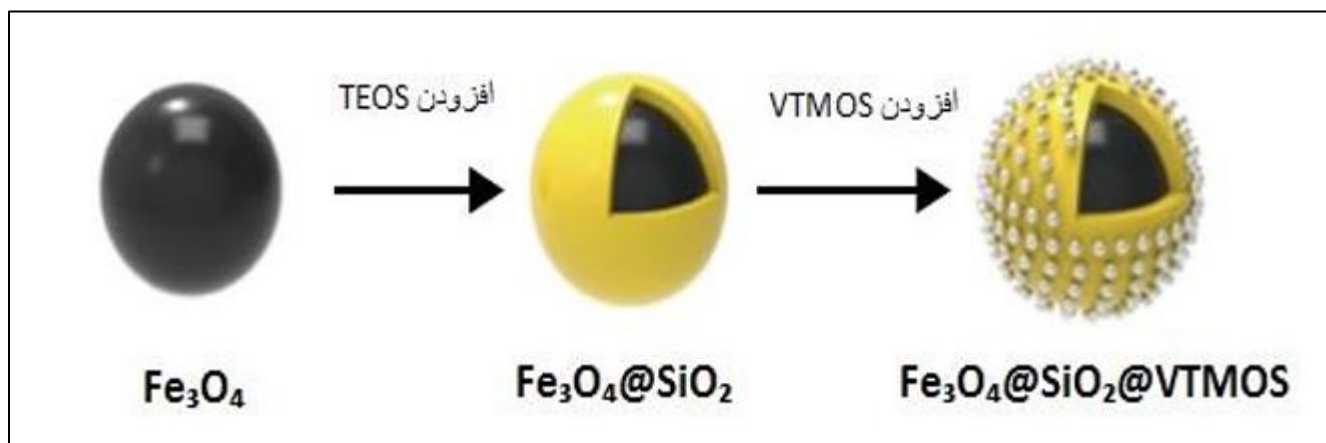


Fig 9: Steps of Functionalizing Magnetite Nanoparticles with Vinyl Groups

Trimethoxyvinyl silane (VTMOS) was used to place the vinyl group on the surface of  $Fe_3O_4$ . During this reaction, the methoxy groups related to the removal and attachment agent of the vinyl silane group are placed on the surface of SCMNPs.

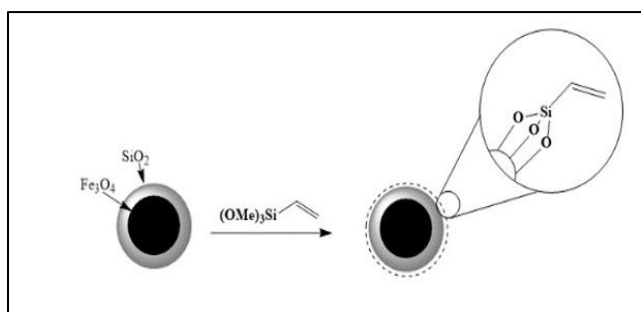


Fig 10: A Scheme of SCMNPs Vinylation Process

➤ *Examination of the Infrared Pattern (FT-IR) related to Vinyl( $Fe_3O_4@SiO_2$ )*

All the bands related to the previous steps can also be seen in the spectrum of  $Fe_3O_4@SiO_2$ . In this spectrum, the band related to vinyl groups appeared at  $1645\text{cm}^{-1}$ .

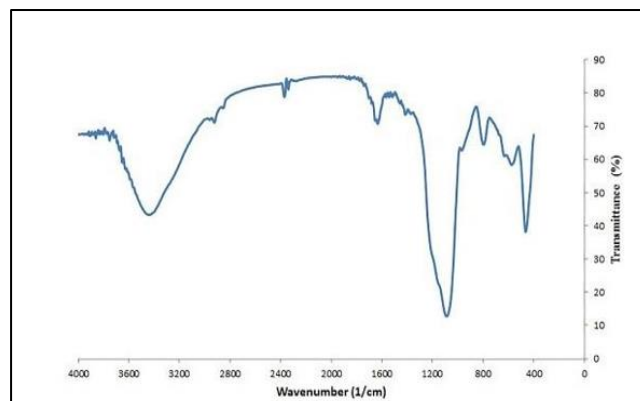


Diagram 4: FT-IR Spectrum of  $Fe_3O_4@SiO_2@Vinyl$

*D. Extraction of Hydrogel of Plantago Ovata*

In order to extract Plantago ovata hydrocolloid for use in the production of magnetic nanocapsules, 50 grams of Plantago ovata seeds were ground for 2 minutes by a laboratory mill, and then the bran was separated from the kernel using a laboratory sieve (mesh 20). The yield after grinding and sieving was about one-third of the initial weight of Plantago ovata seeds (17 grams).

To obtain the hydrogel of Plantago ovata, 30 times the weight of bran (500 ml) was added to distilled water and it was allowed to remain at room temperature for 24 hours. After that, 96% ethanol was added to the mixture in the amount of 3 times the volume of the obtained gel, so that the gel remained suspended in the solution. The resulting sediment was washed 3 times with ethanol, and then it was ground with a Porcelain mortar to perform other tests (47). The obtained gel powder was identified by FT-IR spectroscopy. In addition, the swelling rate of this hydrogel was investigated at different pH (4.2, 7.4, 9.0).



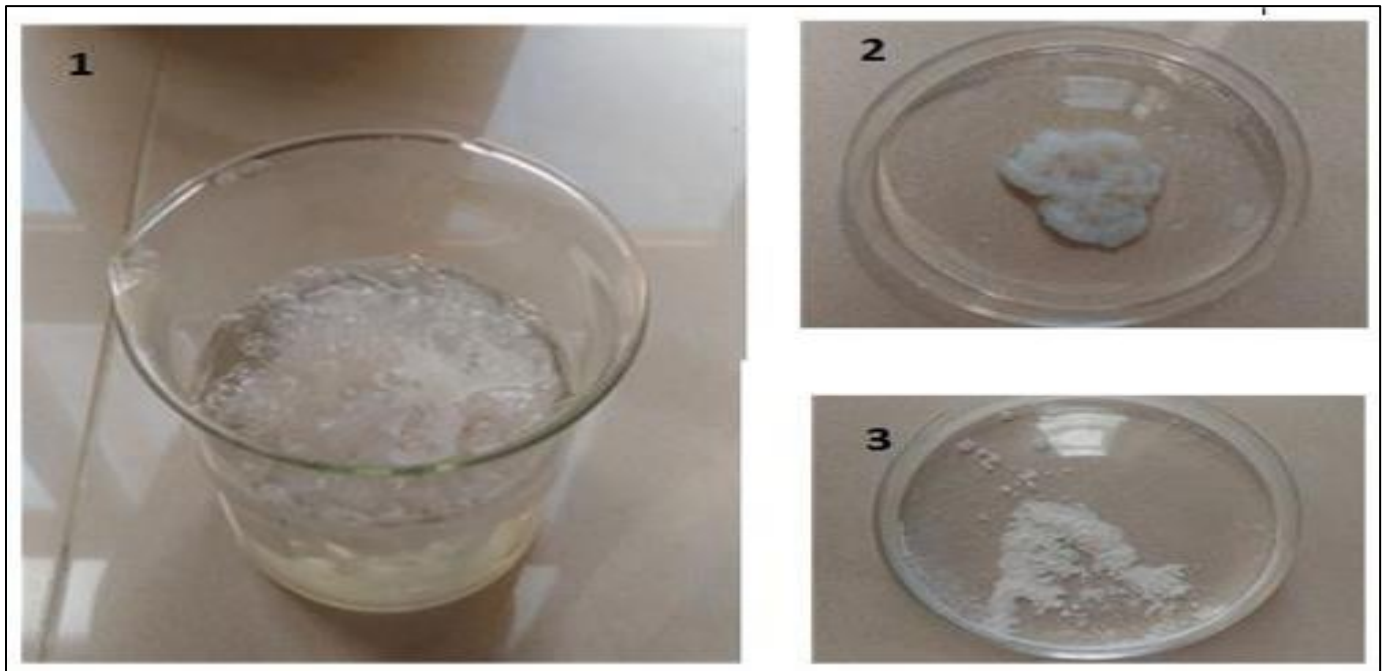


Fig 11: Steps of extracting Plantago Ovata Gel Powder in the Laboratory

➤ *Identification of the Hydrogel Extracted from Plantago Ovata*

Mucilage or fibrous and white part that can be extracted from the bran of Plantago ovata and is the main factor of water absorption in this plant. Its main ingredient is neutral arabinoxyylan.

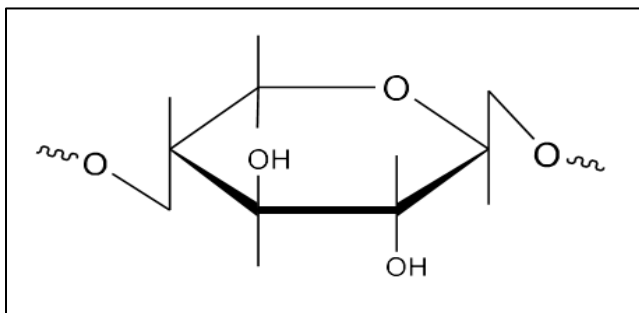


Fig 12: The Structure of the Main Component in Plantago Ovata Mucilage

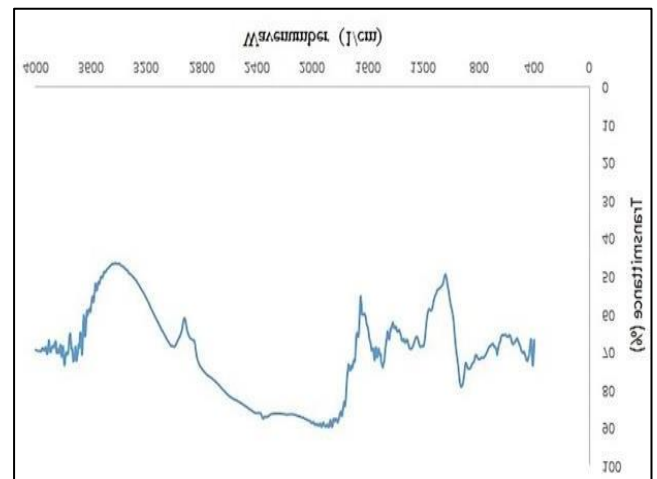


Diagram 5: FT-IR Spectrum Obtained from Plantago Ovata Hydrogel

➤ *Investigation of the FT-IR Spectrum Obtained from Plantago Ovata Hydrogel*

The band related to stretching vibrations of C—O—C bonds can be seen in the range of 1040 $\text{Cm}^{-1}$ . The band seen around  $\text{Cm}^{-1}2900$  is also related to the CH alkyl stretching vibrations in the compound. Also, the broad band appearing at 3400 $\text{Cm}^{-1}$  is related to the stretching vibration of O—H bonds in the compound.

*E. Investigating the Swelling Rate of Plantago Ovata Gel Powder at Different pHs*

After preparing three acidic, basic and neutral solutions (Ph = 2.4, 4.7, 9), the resulting gel powder was added in equal proportion to all three solutions and after one hour and complete swelling, the excess solvent was removed by filter paper. The results of the investigation of the swelling of the Plantago ovata in three acidic, neutral and alkaline environments are shown in diagram 6. As can be seen, the highest amount of swelling is related to the neutral solvent (pH=4.7). This feature can be considered as one of the merits of this natural hydrogel for targeted pharmaceutical systems.

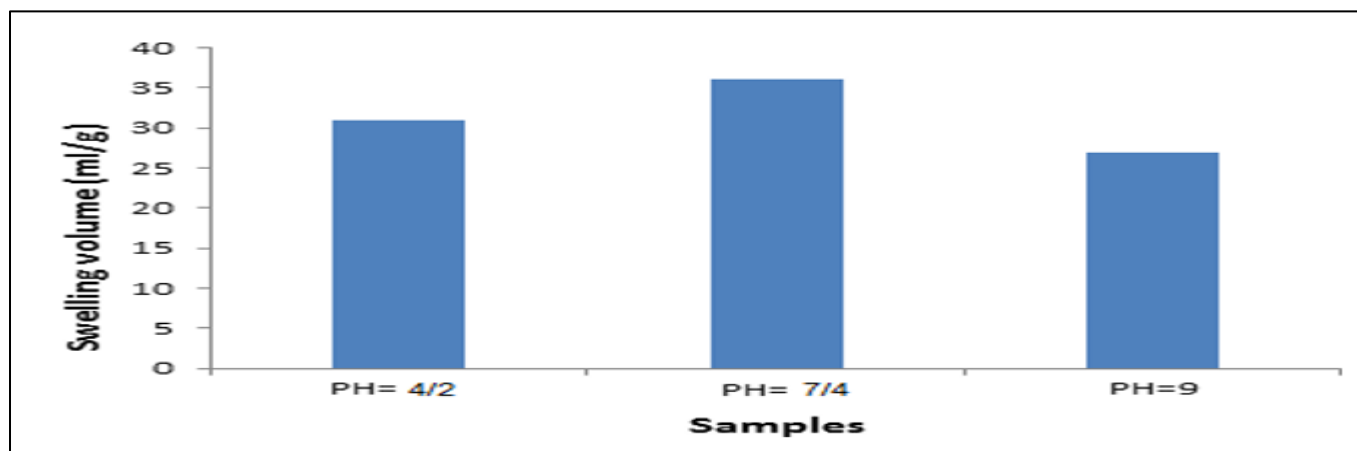


Diagram 6: Investigating the Amount of Swelling of Plantago Ovata Powder in Different pH

#### F. Preparation of Natural Gel Powder Functionalized by Trimethoxyvinyl Silane Groups (Psy@Vinyl)

In a 100 ml double-mouth flask, 0.5 g of gel powder extracted from the mucilage of Plantago ovata seed was poured with 50 ml of distilled water, this mixture was stirred for 15 minutes by a magnetic stirrer. Then 5 ml of VTMOs substance was added drop by drop to the mixture, the reaction was refluxed for 24 hours and then dried in a laboratory oven at 60°C. The product was identified by FT-IR spectroscopy.

#### ➤ FT-IR Spectrum of the Hydrogel Obtained from Functionalized Spore with Vinyl Groups

As shown in Figure 7, all the bands observed in the FT-IR spectrum of the hydrogel extracted from the e Plantago ovata peel (previous step) can also be seen in this spectrum. In addition, the band appearing at 800  $\text{cm}^{-1}$  is related to the Si-O bond and indicates the presence of silicon group in the composition; the band related to stretching vibrations of Si-OMe bonds also appeared in the range of 1000-1100  $\text{cm}^{-1}$ . The presence of C=C groups in the compound is also confirmed by the bands appearing at 1600  $\text{cm}^{-1}$ .

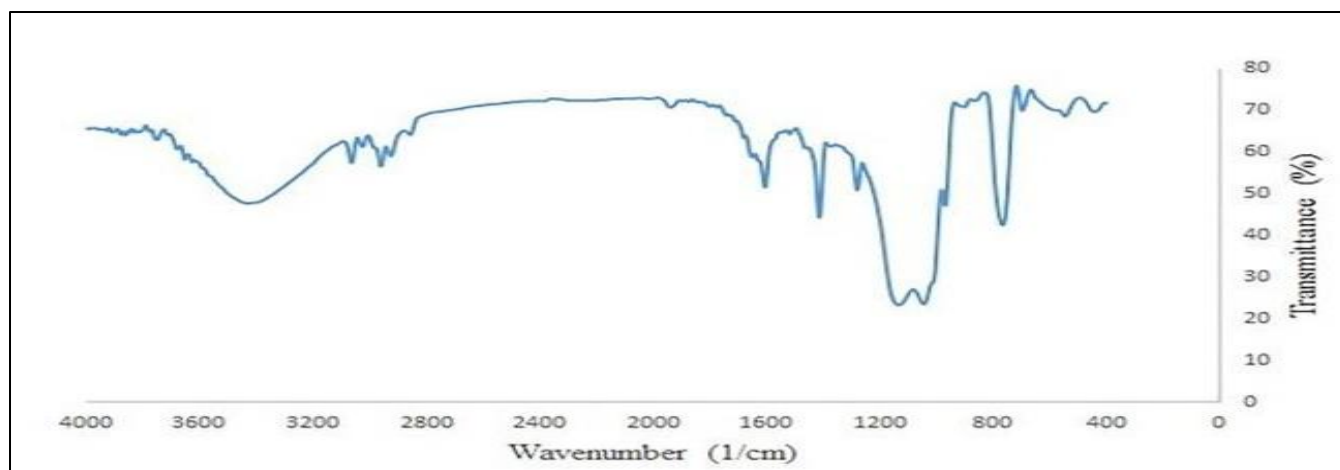


Diagram 7: FT-IR Spectrum Related to Hydrocolloid Functionalized with Vinyl Groups

#### G. Review of FT-IR Spectrum Obtained from Pure Mefenamic Acid Drug

In order to study the final product and identify the bands related to mefenamic acid drug, FT-IR spectrum was taken from the drug and the result is shown in diagram 8. The band related to stretching and bending vibrations of NH group appeared in the range of 3400  $\text{cm}^{-1}$  and 1647  $\text{cm}^{-1}$ ,

respectively. The bands seen in the range of 1446  $\text{cm}^{-1}$ , 1504  $\text{cm}^{-1}$  and 1571  $\text{cm}^{-1}$  are also related to the stretching vibrations of the aromatic rings in the compound. Also, the bands at 1253  $\text{cm}^{-1}$  and at 1600  $\text{cm}^{-1}$  are related to bending vibrations of OH groups and stretching vibrations of C=O group, respectively.

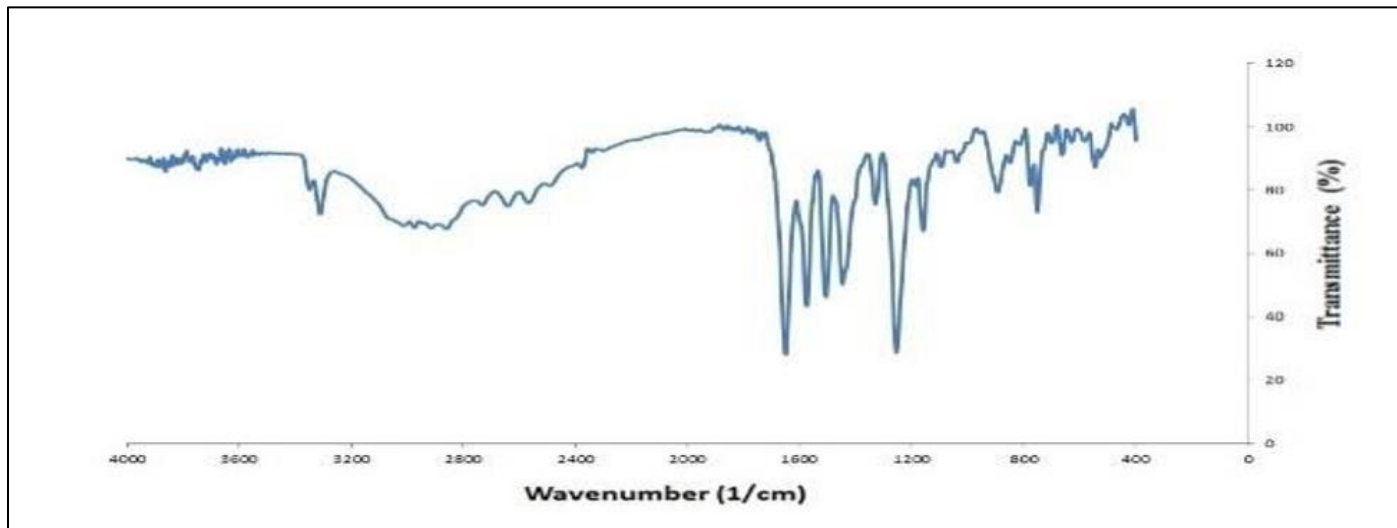


Diagram 8: FT-IR Spectrum Obtained from Mefenamic Acid Drug

#### H. Preparation of the final product

##### *(Fe<sub>3</sub>O<sub>4</sub>@SiO<sub>2</sub>@Psy@drug)*

In a 250 ml Erlenmeyer flask, 0.2 g of Fe<sub>3</sub>O<sub>4</sub> nanoparticles functionalized with vinyl groups (Fe<sub>3</sub>O<sub>4</sub>@SiO<sub>2</sub>@Vinyl) along with 60 ml of absolute ethanol were poured and stirred for 15 minutes by a magnetic stirrer until the nanoparticles are completely uniformly dispersed in the solution. Then 0.6 grams of natural polymer modified with vinyl (Psy@Vinyl) and 102 microliters of methacrylic acid (MAA) (equivalent to 0.6 mmol) were added to the contents of Erlen-meyer. The mixture was placed in an ultrasonic bath for 15 minutes. The obtained solution was poured into a two-hole balloon in a hot water bath with a temperature of 70 °C. The flow of nitrogen gas was directed into the solution to remove the oxygen dissolved in the environment. After 12 hours, 230 microliters of ethylene glycol dimethacrylate (EGDMA) (0.6 mmol) were added to create cross-links between polymer strands in the hydrogel and 2 mg of azobisisobutyronitrile (AIBN) (0.01 mmol) as an initiator. It was added to the mixture inside the container and at the same time, a solution of mefenamic acid in absolute ethanol (with a concentration of 1 gram in 60 ml) was added to the reaction medium so that the drug is trapped in the created networks at the same time as the polymerization and cross-linking are carried out. Finally, the mixture was refluxed with nitrogen for 24 h. The resulting product was separated from the liquid phase by a magnet and washed several times

with acetic acid: methanol (1:9). The resulting sediment was dried in a vacuum oven at a temperature of 40 °C. The product was identified by FT-IR spectroscopy and its morphology was examined by SEM image.

#### ➤ Examination of the Infrared Pattern of the Final Product (FT-IR)

The FT-IR spectrum obtained from the product composition is shown in Figure (4-10). According to the band appearing at 453 cm<sup>-1</sup>, which is related to stretching vibrations of the Fe-O bond, the existence of a magnetic core in the composition of the product is confirmed, in addition to that, the bands appearing at 760 cm<sup>-1</sup> and 1070 cm<sup>-1</sup> are also related to Si-O-Si vibrations and indicates the presence of silica in the composition. The band at 1250 cm<sup>-1</sup> is also related to the stretching vibrations of C—O and C—O—C bonds and indicates the presence of arabinosyran molecules in the natural polymer obtained from *Plantago ovata*. The bands appearing in 1434 cm<sup>-1</sup>, 1500 cm<sup>-1</sup>, and 1571 cm<sup>-1</sup> are related to the vibrations of the benzene ring, which indicates the presence of the drug in the compound, and the band in 3308 cm<sup>-1</sup> is also related to the amino group of the drug compound. At 2900 cm<sup>-1</sup>, the band corresponding to the alkane CHs of the compound has also appeared. The obtained spectrum indicates that the product has been prepared correctly.

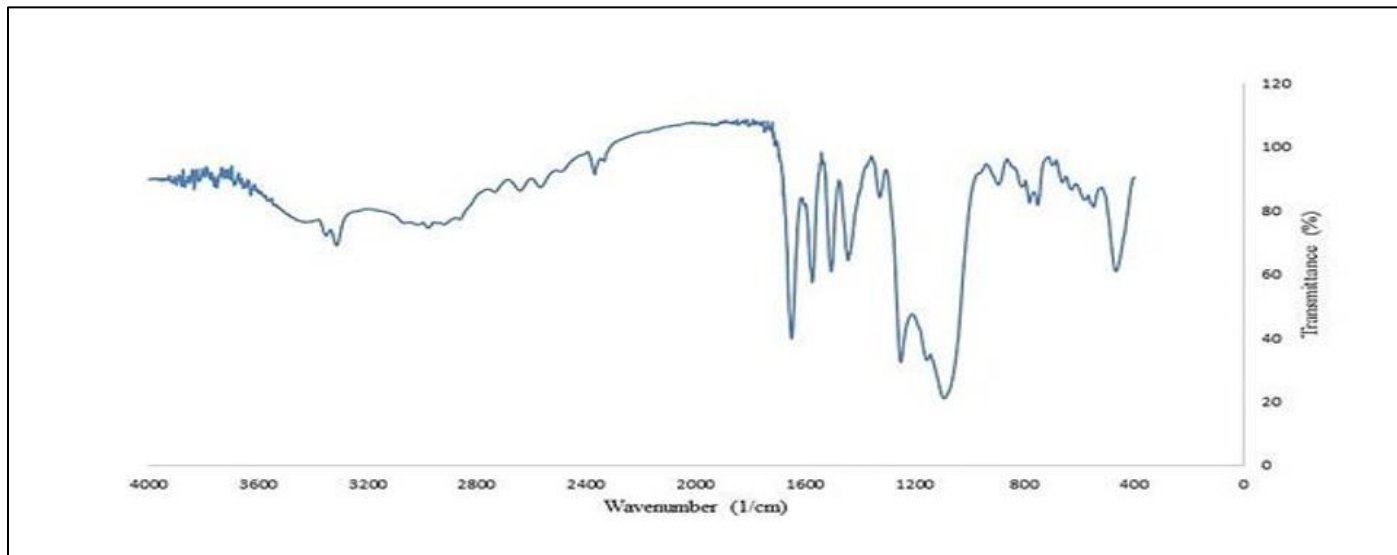


Diagram 9: FT-IR Spectrum Obtained from the Final Product

➤ *Examining Magnetometric Analysis of the Final Product (VSM)*

The magnetic behavior of the final product was investigated using VSM analysis. The result of the magnetization analysis shown in Figure 10 shows the absence of a hysteresis loop in the composition and a confirmation of

its superparamagnetic behavior. Despite the decrease in magnetization to 25 emu/g, which is due to the presence of silica layer and natural polymer as well as mefenamic acid drug, the superparamagnetic property of the compound is preserved.

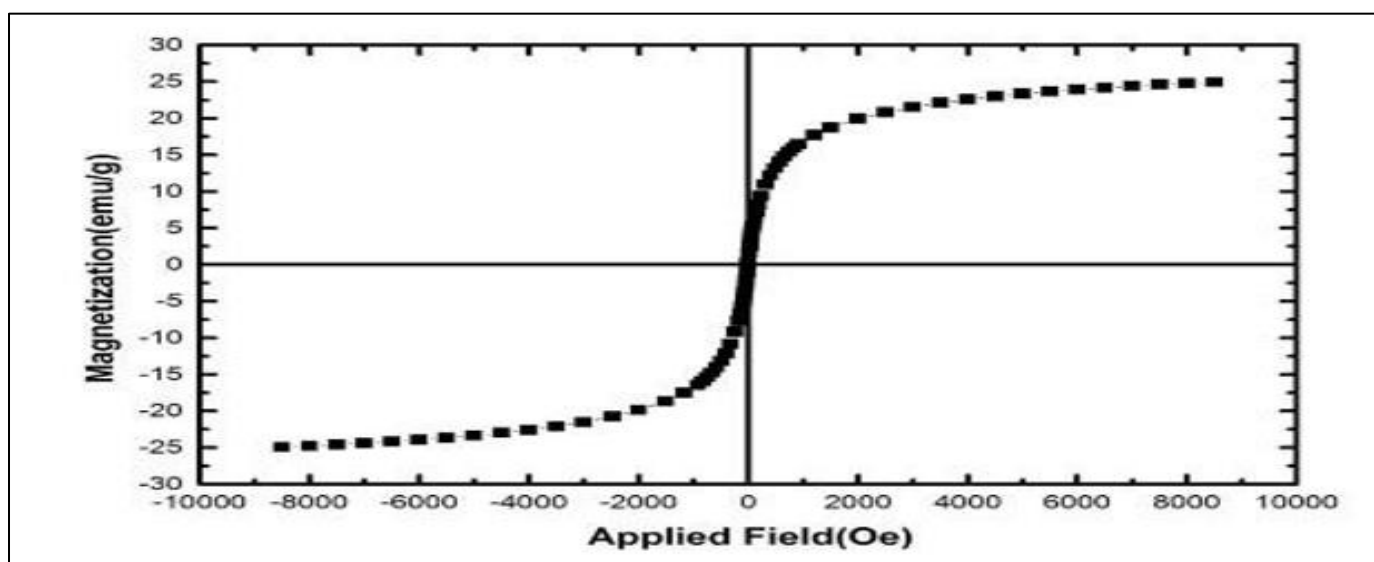


Diagram 10: VSM Analysis Obtained from the Final Product

➤ *Examining the X-Ray Diffraction Pattern of the Final Product (XRD)*

Diagram 11 shows the X-ray diffraction pattern of the composition of the product obtained from the previous steps. Comparing this pattern with the pattern related to the composition of  $\text{Fe}_3\text{O}_4$ , which is given in diagram 11, shows that in addition to the diffractions related to the magnetite structure, a wide diffraction is observed in the  $\theta$ 2 region equal to 20, which was determined by referring to the available

sources that the existing diffraction is related to the structure of the *Plantago ovata* mucilage [22].

In addition, diffractions in the  $\theta$ 2 region equal to 14.3 and 26.3 are seen, and the existence of the mentioned diffractions is consistent with the pattern related to mefenamic acid in the sources and it is a confirmation of the stabilization of mefenamic drug on  $\text{Fe}_3\text{O}_4$  magnetic nanoparticles and the formation of the desired compound (23).



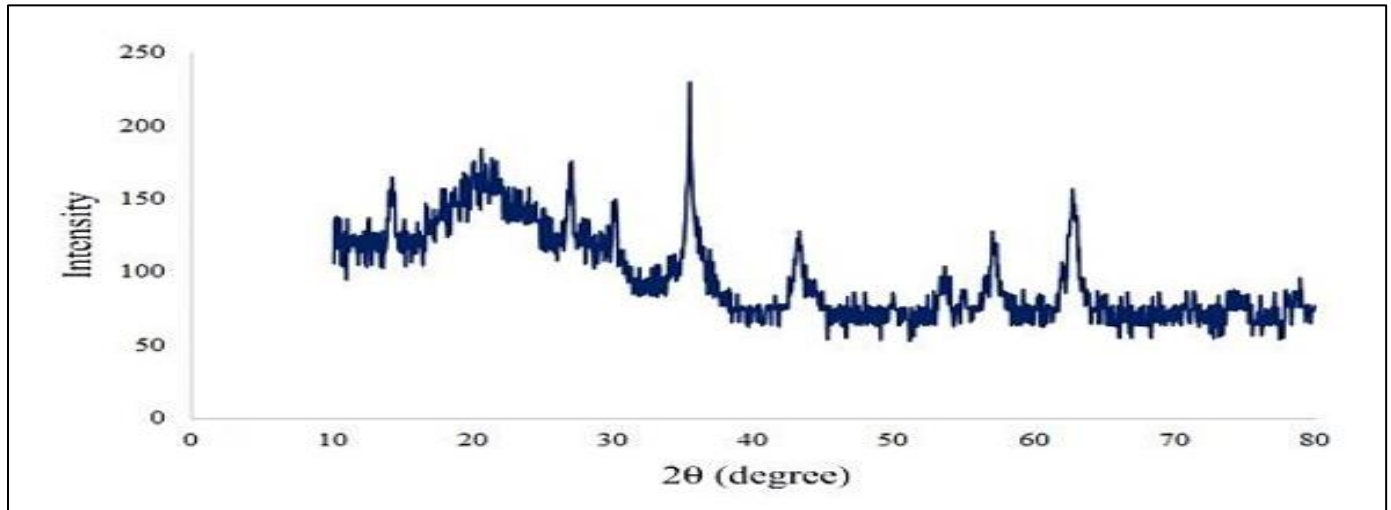


Diagram 11: XRD Analysis Obtained from the Final Product

➤ *Review of DLS Analysis*

Dynamic light scattering is a physical method used to determine the distribution of particles in solutions and suspensions. This non-destructive and fast method is used to determine the size of particles in the range of several nanometers to microns. In recent technologies, particles with a diameter of less than nanometers can also be measured with this method. This method depends on the interaction of light with the particle. The light scattered by the nanoparticles in the

suspension changes with time, which can be related to the particle diameter. Figure 12 shows the results of the DLS test of the product sample. The size of the particles has a significant effect in controlling the responses of the biological environment, such as immunogenicity, their half-life, the ability to enter different cells and the targeting of the particles (25). Figure 12 shows the average particle size distribution, which is below 100 nm and is an important parameter for passing through biological cells.

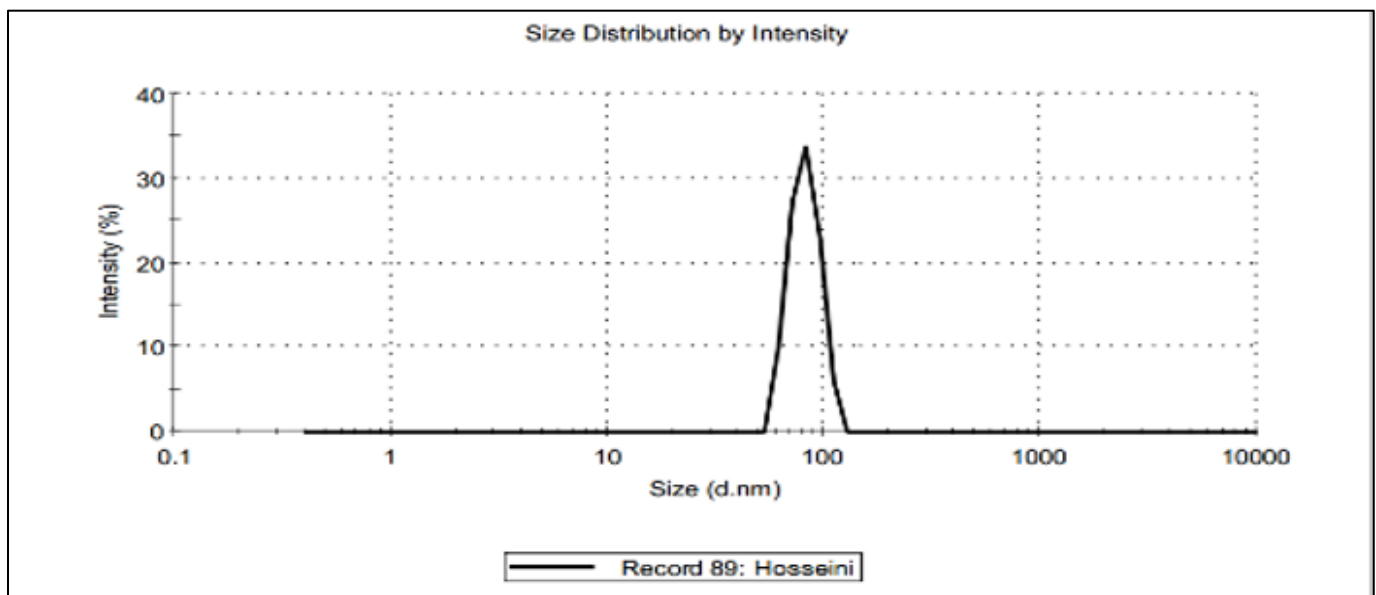


Fig 12: Examining Particle Size Distribution by DLS Analysis

➤ *The Results of the Scanning Electron Microscope (SEM) Test Obtained from the Product*

Figure 13 shows the FE-SEM images of the composition. Compared to the FE-SEM images related to the Fe<sub>3</sub>O<sub>4</sub> composition shown in Figure 13, it can be seen that the

size of the nanoparticles has increased, which is due to the presence of the polymer layer and the loading of the drug in it, the size of the obtained nanoparticles is about nm is 40-50.

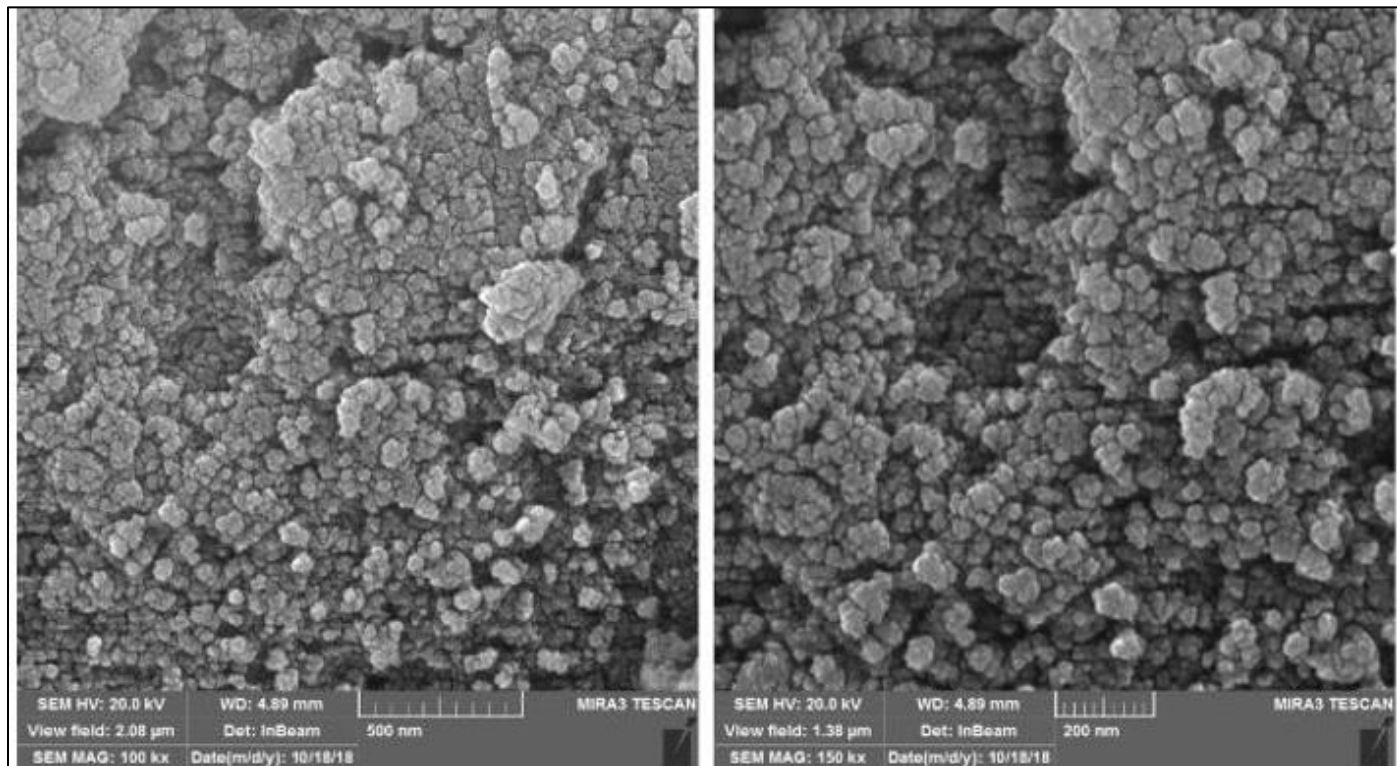


Fig 13: SEM Images Obtained from the Final Product

#### ➤ Examining the Thermal Stability of the Product (TGA)

In order to check the thermal stability of the compound, TGA analysis was performed under nitrogen atmosphere and with a temperature gradient of 10 °C per minute, and the results obtained are shown in diagram 13.

The diagram shows several consecutive slopes, which show that the desired composition loses weight in several stages. The first stage of weight loss starts from 50 °C and continues until about 100 °C, this weight loss can be attributed to the loss of water and moisture in the sample. Visible slopes in the range of 200-400 can also be attributed to the degradation of organic compounds in the sample (polymeric groups and loaded mefenamic acid drug).

The second slope, starting at 150 °C and ending at 300 °C, leads to a 15% reduction in sample weight. At a temperature above 300 °C, organic compounds begin to decompose more steeply. This stage continues up to 400°C and causes a 35% reduction in the weight of the sample. The information obtained from the analysis of the thermal decomposition of the sample confirms the presence of several groups of organic substances in the composition of the product, which are loaded on the Fe<sub>3</sub>O<sub>4</sub> substrate. The results are in good agreement with the information obtained from previous analyses.

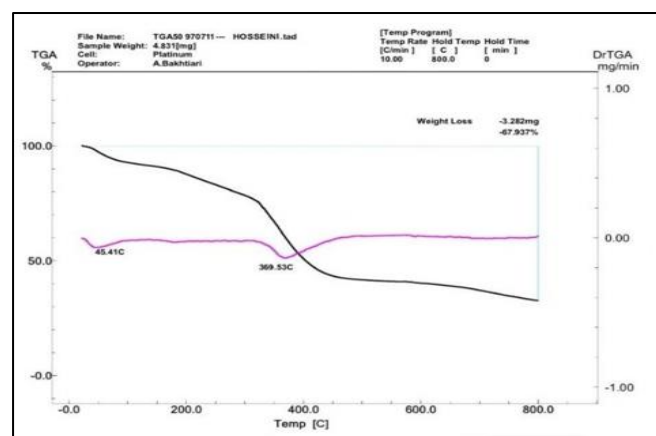


Diagram 13: Thermal Decomposition Analysis of the Final Product

#### ➤ Investigation of the Release of Mefenamic Acid Drug from Polymer Networks

In figure 14, the absorption spectrum of mefenamic acid drug is given, as it can be seen, the spectrum of mefenamic acid has two absorption bands in the range of 281 nm and 349 nm, before studying the absorption of standard solutions to draw a calibration chart, the absorption of natural hydrogel extracted from *Plantago ovata* was checked to investigate the non-interference of the absorption bands of the drug with the hydrogel.

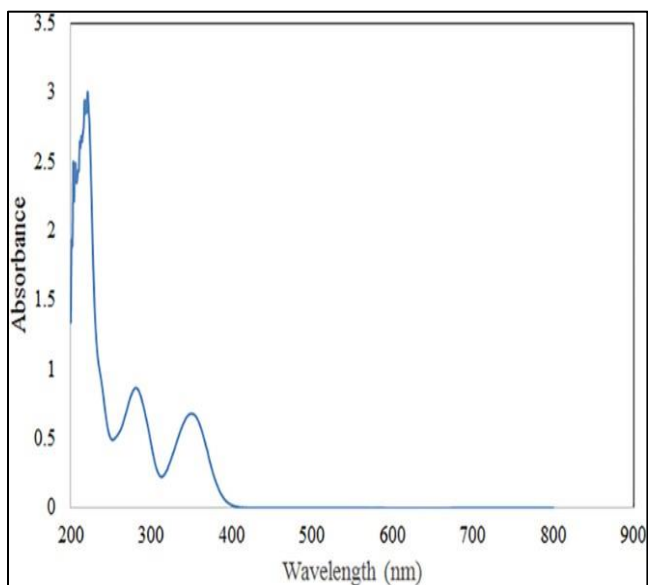


Fig 14: UV-Vis Absorption Spectrum of Pure Mefenamic Acid Drug

As can be seen in the figure below, the spectrum of natural hydrogel has only one absorption band in the 276 nm range. Due to the possibility of interference between the absorption bands of the hydrogel and the absorption band of the drug at 281 nm, the absorption band at 349 nm of the drug was used to draw the calibration graph and study the drug release.

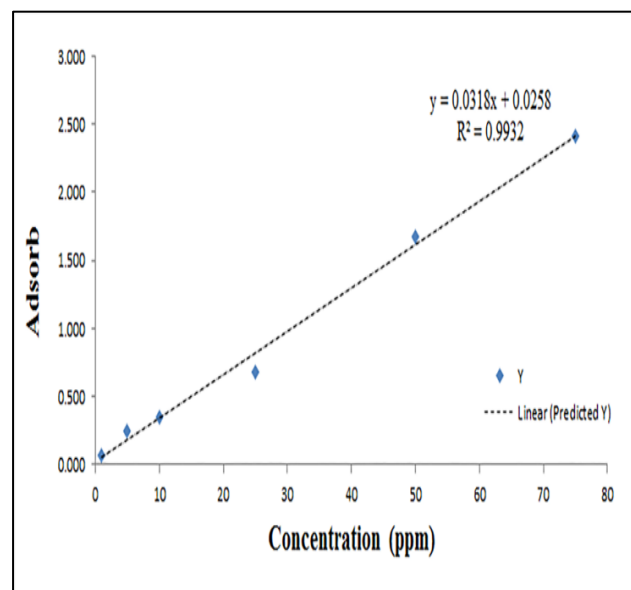


Diagram 14: Mefenamic Acid Drug Calibration Graph

By investigation the amount of absorption of the solution, the result of the mass of the remaining drug (unencapsulated) was 0.36 grams. As a result, the amount of drug loading is 64%.

$$64\% = 100 \times 1 / (1 - 0.36) = \text{encapsulation efficiency.}$$

Also, the release of mefenamic acid drug trapped in polymer networks is shown in diagram 15. This investigation was done within 72 hours and in a blood plasma simulating solution (phosphate buffer pH: 4.7). According to the diagram, the drug release pattern from the polymer networks had an upward trend in the first 8 hours and approximately 35% of the loaded drug was released, after that the release slope continued with a milder range for 26 hours. And finally, this process is almost fixed.

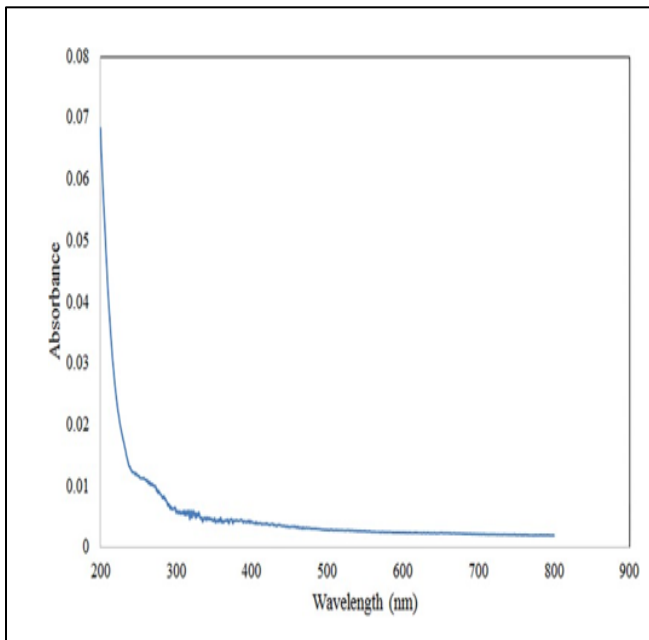


Fig 15: UV-Vis Absorption Spectrum of Plantago Ovata Natural Hydrosol

Chart 14 shows concentration calibration according to drug. The equation of the line and the degree of reaction error are also given. As can be seen in the diagram, the obtained regression coefficient is 0.9932, which indicates the high accuracy of the work in the stages of sample preparation.

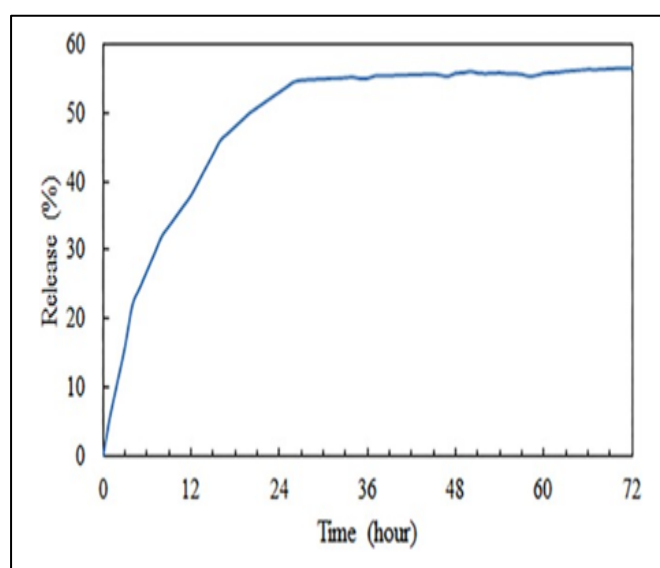


Diagram 15: Diagram of Mefenamic Acid Drug Release from Magnetic Hydrogel

### I. Examining the efficiency of drug loading

To examine the amount of drug loading and encapsulation, at first, the final synthesized product was isolated by external magnetic field, then it was washed several times with methanol. After separating the solid phase, the collected residual liquid was used to take the UV test from it and obtain the amount of unloaded drug. For this purpose, after reading the absorbance in the wavelength range of mefenamic acid drug (349 nm) and finding the concentration of free drug in the environment (unencapsulated drug) using the equation of the calibration graph line and calculating its weight percentage, The concentration of the drug that is free in the environment and not encapsulated is obtained. Next, by subtracting this amount from the total mass of the drug used for encapsulation and dividing it by the total mass of the drug, the drug loading efficiency and the encapsulation efficiency are obtained.

$100 \times (\text{initial mass of drug used}) / (\text{mass of free drug in the environment} - \text{initial mass of drug used}) = \text{encapsulation efficiency}$  6- 10. Drug release from hydrogel Drug release from natural polymer networks was investigated using an ultraviolet- visible spectrometer. For this purpose, in accordance with Beer-Lambert law, solutions with different drug concentrations (75, 50, 25, 10, 5, 1 ppm) were prepared and their absorbance was measured at 349 nm wavelength and its calibration curve and equation were drawn.

The release rate of mefenamic acid drug from magnetized polymer was investigated by membrane diffusion technique [26]. 0.2 grams of the prepared final product ( $\text{Fe}_3\text{O}_4 @ \text{SiO}_2 @ \text{Psy} @ \text{drug}$ ) was poured into a dialysis bag (Sigma Aldrich) containing 0.5 ml of buffer solution (pH=4.7) and poured into a 200 ml beaker. It was suspended from the same buffer, and the beaker content was stirred using a magnetic stirrer until the end of the release process. With the passage of time, the buffer inside the bag penetrated the hydrogel, which caused swelling and subsequent destruction of the hydrogel. This action caused the gradual release of the drug from the nanoparticles, and subsequently, the increase in its concentration in the buffer solution. At specific time intervals (1 hour, 2 hours, 4 hours, 8 hours and 12 hours), 2 ml of the resulting solution was placed in the UV-Vis device to measure absorption. It is necessary to explain that the volume subtracted from beaker contents was compensated by adding fresh buffer, thus the buffer volume remained constant during sampling. Next, using the calibration curve that was drawn before, the concentration of mefenamic acid drug released at anytime was calculated, and using the obtained information, the drug release graph was drawn according to time.

## V. CONCLUSION

Natural polysaccharides are suitable options for use as drug carriers due to their advantages such as their high biocompatibility in the body environment, their non-toxicity and their cheapness. In addition to its benefits in solving problems of the digestive system and reducing blood cholesterol, the mucilage extracted from the shell of *Plantago ovata* can be used as a natural drug carrier in drug delivery systems due to its cross-links and network

In this research, an attempt has been made to provide a method for encapsulating the drug, during which the drug can be controlled and targeted by the magnetic field.

Examining the obtained results indicates that the natural polymer is correctly loaded on the desired magnetic substrate and the mefenamic acid drug is trapped inside the hydrogel networks and polymer capsule.

The results of the drug release study from the polymer capsule indicate that the drug release is done well and at an acceptable speed.

The results of FE-SEM images show that the obtained product had a spherical morphology and the particle size distribution was less than 100 nm. The spherical and symmetrical shape of these particles can help them move in the liquid environment.

Thermal decomposition analysis of the final product also indicates the presence of both organic and inorganic substances in the sample, which is related to the polymer part, the drug part and the magnetic part of the sample.

The results of studies on the swelling of the mucilage removed from the *Plantago ovata* shell at different pHs indicate that the maximum amount of absorption is by *Plantago ovata* polysaccharide in a neutral environment.

## REFERENCES

- [1]. Jain KK. Drug delivery systems-an overview. Drug delivery systems. 2008:1-50.
- [2]. Saltzman WM. Drug delivery: engineering principles for drug therapy. Oxford University Press; 2001 Mar 15.
- [3]. Perrie Y, Rades T. FASTtrack Pharmaceuticals: drug delivery and targeting. Pharmaceutical press; 2012.
- [4]. Tai T, Ho L. Formulating detergents and personal care products. a complete guide to product development.
- [5]. McCredie R, Whistler RL. Quince seed, psyllium seed and flaxseed gums. Industrial Gums, 2nd Ed., RL Whistler and JN BeMiller (eds.) Academic. 1965:433-57.
- [6]. Juturu V, Gormley JJ. Bioactive nutrients and cardiovascular disease. In Bioactive food as dietary interventions for cardiovascular disease 2013 Jan 1 (pp. 73-88). Academic Press.
- [7]. Thakur VK, Thakur MK. Recent trends in hydrogels based on psyllium polysaccharide: a review. Journal of Cleaner Production. 2014 Nov 1;82:1-5.
- [8]. Yun YH, Lee BK, Park K. Controlled Drug Delivery: Historical perspective for the next generation. Journal of Controlled Release. 2015 Dec 10;219:2-7.
- [9]. Masserini M. Nanoparticles for brain drug delivery. International Scholarly Research Notices. 2013;2013.
- [10]. Hamidi M, Azadi A, Rafiei P. Hydrogel nanoparticles in drug delivery. Advanced drug delivery reviews. 2008 Dec 14;60(15):1638-49.



- [11]. Arias JL, editor. Nanotechnology and drug delivery, volume one: nanoplateforms in drug delivery. CRC Press; 2014 Aug 4.
- [12]. Kandpal ND, Sah N, Loshali R, Joshi R, Prasad J. Co-precipitation method of synthesis and characterization of iron oxide nanoparticles.
- [13]. Mascolo MC, Pei Y, Ring TA. Room temperature co-precipitation synthesis of magnetite nanoparticles in a large pH window with different bases. *Materials*. 2013 Nov 28;6(12):5549-67.
- [14]. Hariani PL, Faizal M, Setiabudidaya D. Synthesis and properties of Fe<sub>3</sub>O<sub>4</sub> nanoparticles by co-precipitation method to removal procion dye. *International Journal of Environmental Science and Development*. 2013 Jun 1;4(3):336.
- [15]. Bhattarai N, Gunn J, Zhang M. Chitosan-based hydrogels for controlled, localized drug delivery. *Advanced drug delivery reviews*. 2010 Jan 31;62(1):83-99.
- [16]. Kreuter J, Ramge P, Petrov V, Hamm S, Gelperina SE, Engelhardt B, Alyautdin R, Von Briesen H, Begley DJ. Direct evidence that polysorbate-80-coated poly (butylcyanoacrylate) nanoparticles deliver drugs to the CNS via specific mechanisms requiring prior binding of drug to the nanoparticles. *Pharmaceutical research*. 2003 Mar;20:409-16.
- [17]. Wichterle O, Lim D. Hydrophilic gels for biological use. *Nature*. 1960 Jan 9;185(4706):117-8.
- [18]. Cimolai N. The potential and promise of mefenamic acid. *Expert review of clinical pharmacology*. 2013 May 1;6(3):289-305.
- [19]. Teja AS, Koh PY. Synthesis, properties, and applications of magnetic iron oxide nanoparticles. *Progress in crystal growth and characterization of materials*. 2009 Mar 1;55(1-2):22-45.
- [20]. Liu X, Ma Z, Xing J, Liu H. Preparation and characterization of amino-silane modified superparamagnetic silica nanospheres. *Journal of Magnetism and magnetic Materials*. 2004 Mar 1;270(1-2):1-6.
- [21]. Saadati-Moshtaghin HR, Zonoz FM. Preparation and characterization of magnetite-dihydrogen phosphate as a novel catalyst in the synthesis of tetrahydrobenzo
- [22]. [b] pyrans. *Materials Chemistry and Physics*. 2017 Sep 15;199:159-65.
- [23]. Gill CS, Price BA, Jones CW. Sulfonic acid-functionalized silica-coated magnetic nanoparticle catalysts. *Journal of Catalysis*. 2007 Oct 1;251(1):145-52.
- [24]. Yamaura M, Camilo RL, Sampaio LC, Macêdo MA, Nakamura M, Toma HE. Preparation and characterization of (3-aminopropyl) triethoxysilane-coated magnetite nanoparticles. *Journal of magnetism and magnetic materials*. 2004 Aug 1;279(2-3):210-7.
- [25]. Takami S, Sato T, Mousavand T, Ohara S, Umetsu M, Adschiri T. Hydrothermal synthesis of surface-modified iron oxide nanoparticles. *Materials Letters*. 2007 Oct 1;61(26):4769-72.
- [26]. Zou LQ, Liu W, Liu WL, Liang RH, Li T, Liu CM, Cao YL, Niu J, Liu Z. Characterization and bioavailability of tea polyphenol nanoliposome prepared by combining an ethanol injection method with dynamic high-pressure microfluidization. *Journal of Agricultural and Food Chemistry*. 2014 Jan 29;62(4):934-41.
- [27]. Wang C, Mallela J, Garapati US, Ravi S, Chinnasamy V, Girard Y, Howell M, Mohapatra S. A chitosan-modified graphene nanogel for noninvasive controlled drug release. *Nanomedicine: Nanotechnology, Biology and Medicine*. 2013 Oct 1;9(7):903-11.
- [28]. Mokri SM, Valadbeygi N, Stelnikova IG. Using Convolutional Neural Network to Design and Predict the Forces and Kinematic Performance and External Rotation Moment of the Hip Joint in the Pelvis. *International Journal of Innovative Science and Research Technology (IJISRT) IJISRT24FEB1059*. 2024:878-83.
- [29]. Valadbeygi N. A Parametric Study to Predict Wind Energy Potential from Neural Network.
- [30]. Mokri SM, Valadbeygi N, Grigoryeva V. Diagnosis of Glioma, Meningioma and Pituitary brain tumor using MRI images recognition by Deep learning in Python. *EAI Endorsed Transactions on Intelligent Systems and Machine Learning Applications*. 2024 Apr 15;1.
- [31]. Valadbeygi N. Wet Cooling Tower Heat Transfer and Function Prediction using MLP Neural Network.
- [32]. Mokri SM, Valadbeygi N, Balyasimovich KM. Predicting the Performance and Adaptation of Artificial Elbow Due to Effective Forces using Deep Learning".
- [33]. Mokri SM, Valadbeygi N, Mohammed K. Physiological study of joint loaded force in the artificial knee with the neural approach.
- [34]. Valadbeygi N, Shahrjerdi A. Prediction of Heating Energy Consumption in Houses via Deep Learning Neural Network. *Analytical and Numerical Methods in Mechanical Design*. 2022 Dec 1;1(2):11-6.
- [35]. Hosseini V, Mokri SM, Viktorovna KA. Targeted Drug Delivery through the Synthesis of Magnetite Nanoparticle by Co-Precipitation Method and Creating a Silica Coating on it.